Nutrition & Metabolism

RESEARCH

Open Access

Metabolic profiles and prediction of failure to thrive of citrin deficiency with normal liver function based on metabolomics and machine learning

Peiyao Wang[1†], Duo Zhou[1†], Lingwei Hu[1†], Pingping Ge[1], Ziyan Cen[1], Zhenzhen Hu[1], Qimin He[2,3*], Kejun Zhou[4*], Benqing Wu[5,6*] and Xinwen Huang[1*]

Abstract

Purpose This study aimed to explore metabolite pathways and identify residual metabolites during the post-neonatal intrahepatic cholestasis caused by citrin deficiency (post-NICCD) phase, while developing a predictive model for failure to thrive (FTT) using selected metabolites.

Method A case-control study was conducted from October 2020 to July 2024, including 16 NICCD patients, 31 NICCD-matched controls, 34 post-NICCD patients, and 70 post-NICCD-matched controls. Post-NICCD patients were further stratified into two groups based on growth outcomes. Biomarkers for FTT were identified using Lasso regression and random forest analysis. A non-invasive predictive model was developed, visualized as a nomogram, and internally validated using the enhanced bootstrap method. The model's performance was evaluated with receiver operating characteristic curves and calibration curves. Metabolite concentrations (amino acids, acylcarnitines, organic acids, and free fatty acids) were measured using liquid chromatography or ultra-performance liquid chromatography-tandem mass spectrometry.

Results The biosynthesis of unsaturated fatty acids was identified as the most significantly altered pathway in post-NICCD patients. Twelve residual metabolites altered during both NICCD and post-NICCD phases were identified, including: 2-hydroxyisovaleric acid, alpha-ketoisovaleric acid, C5:1, 3-methyl-2-oxovaleric acid, C18:1OH, C20:4, myristic acid, eicosapentaenoic acid, carnosine, hydroxylysine, phenylpyruvic acid, and 2-methylcitric acid. Lasso regression

†Peiyao Wang, Duo Zhou and Lingwei Hu contributed equally to this work.

*Correspondence:
Qimin He
heqimin@usts.edu.cn
Kejun Zhou
zhoukejun1984@163.com
Benqing Wu
wubenqing783@126.com
Xinwen Huang
6305022@zju.edu.cn

Full list of author information is available at the end of the article

and random forest analysis identified kynurenine, arginine, alanine, and aspartate as the optimal biomarkers for predicting FTT in post-NICCD patients. The predictive model constructed with these four biomarkers demonstrated an AUC of 0.947.

Conclusion While post-NICCD patients recover clinically and biochemically, their metabolic profiles remain incompletely restored. The predictive model based on kynurenine, arginine, alanine, and aspartate provides robust diagnostic performance for detecting FTT in post-NICCD patients.

Keywords Citrin deficiency, Metabolomics, Failure to thrive, Amino acids, Lipids

Introduction

Citrin deficiency (CD) is an autosomal recessive disorder caused by mutations in the *SLC25A13* gene, presenting in three age-dependent clinical phenotypes: neonatal intrahepatic cholestasis caused by citrin deficiency (NICCD), post-NICCD (adaptation or compensation state), and adolescent and adult citrin deficiency (AACD) [1, 2]. CD disrupts the malate-aspartate shuttle, impairing the tricarboxylic acid (TCA) cycle and urea cycle, leading to decreased energy production and metabolic dysfunction [3]. Energy deficit in hepatocytes is the central pathological mechanism of CD, contributing to liver dysfunction, growth impairment, and nutritional problems [4]. Treatment strategies include lactose-restricted formulas, low-carbohydrate diets, and medium-chain triglyceride (MCT) supplementation [5]. MCTs are absorbed independently of bile acids, undergo β-oxidation to rapidly provide energy, promote lipogenesis and glycogenesis, and restore the cytosolic NAD+/NADH ratio, making it a potential therapeutic option for alleviating energy deficits and improving growth and clinical outcomes [6, 7].

Patients with NICCD generally respond well to treatment, significantly improving cholestasis, citrullinemia, and overall health within the first year [6, 8]. While the post-NICCD stage was previously considered "apparently healthy", Saheki et al. [9] demonstrated that this phase can still present clinical symptoms, including failure to thrive (FTT), hyperlipidemia, hepatoma, and pancreatitis. Further research has revealed unique metabolic abnormalities during this stage, including enhanced cholesterol synthesis and elimination in the liver and brain [10], as well as altered amino acid profiles characterized by decreased glucogenic amino acids and increased ketogenic amino acids, branched-chain amino acids (BCAAs), valine intermediates, and β-alanine [11]. Oxidative stress is also elevated during this phase [12]. As a transitional stage between NICCD resolution and potential AACD development, the post-NICCD phase represents a critical window for early intervention to prevent progression to AACD. However, understanding the metabolic profiles in post-NICCD remains limited, particularly regarding key metabolic pathway disruptions and residual metabolite accumulation.

Growth outcomes are key indicators of long-term prognosis in children with CD. Studies have shown that hypoglycemic attacks and growth failure are common manifestations of CD after one year of age [13]. FTT in CD is observed not only during the neonatal period, with low birth weight and length, but also during adolescence, particularly in males [14]. Metabolic disruptions in hepatic glycolysis and de novo lipogenesis lead to energy deficits that hinder normal growth and development in CD [14]. Growth impairment not only affects physical development but is also associated with long-term deficits in cognitive and immune functions [15]. Poor growth trajectories may reflect unresolved metabolic disturbances or suboptimal management of CD. However, the mechanisms behind FTT in post-NICCD remain poorly understood, and metabolic biomarkers for predicting growth outcomes are lacking. This highlights the urgent need to develop a predictive model for the early identification of at-risk post-NICCD patients and to guide personalized management strategies.

Metabolomics offers a powerful approach to understanding disease mechanisms by comprehensively analyzing metabolic profiles. Recent studies have emphasized the potential of metabolomics in exploring genetic and rare metabolic diseases, especially inborn errors of metabolism [16]. One study showed that Gas Chromatography-Mass Spectrometry (GC-MS) analysis of urine metabolomics allows for a more reliable and rapid diagnosis of CD, distinguishing it from other hyperammonemia syndromes through key metabolites such as tyrosine and its derivatives, α-ketoglutaramate, and nucleic acid metabolites such as orotate and uracil [17]. The metabolomic strategy, focusing on free fatty acids, amino acids, and organic acids, was chosen because it has been reported that these metabolites may be associated with metabolic alterations in CD [11, 12].

This study aims to address these gaps by investigating the metabolic characteristics of post-NICCD and identifying metabolic predictors of FTT, thus laying the foundation for targeted interventions to enhance long-term outcomes in children with CD.

Methods

Study subjects

We conducted a single-center case-control study at the Children's Hospital, Zhejiang University School of Medicine, involving 16 NICCD patients, 34 post-NICCD patients, 31 NICCD-matched controls, and 70 post-NICCD matched controls from October 2020 to July 2024. Among the post-NICCD children, 12 were classified as FTT, while the remaining 22 were considered to have normal growth. The Ethical Committee of Children's Hospital, Zhejiang University School of Medicine approved this study (reference number: 2021-IRB-292). Written consent was obtained from parents for sample collection and data publication.

The NICCD patients included in this study met the diagnostic criteria for NICCD [18] and were confirmed by Sanger sequencing identifying mutations in the SLC25A13 gene. The post-NICCD patients had a prior history of NICCD and were in the follow-up phase, with no overt symptoms and liver function having normalized. Exclusion criteria included intrahepatic cholestasis of other etiologies, post-NICCD patients with incomplete clinical or biochemical recovery, and those with other genetic metabolic disorders. Lifestyle factors, including sleep parameters (total sleep duration, night sleep patterns, and nap frequency) and dietary patterns (protein and fat intake, carbohydrate consumption, meal frequency, and consumption of lactose-restricted formulas), were assessed during routine follow-up visits. These factors were comparable between the post-NICCD FTT and normal growth groups, minimizing potential confounding effects on the metabolite profiles. All controls were recruited from children undergoing routine health check-ups at our pediatric health department. The inclusion criteria for controls were:(1) no history of inherited metabolic disorders, (2) no family history of liver disease, and (3) no clinical signs of liver disease or other systemic illnesses during recruitment. We initially identified a larger pool of potential controls (50 for NICCD and 120 for post-NICCD). Given that metabolic parameters are highly age-dependent, strict age- and sex-matching was applied, resulting in an approximate 1:2 case-to-control ratio for both groups.

Clinical data collection

Demographic data, including subjects' age, sex, birth weight, gestational weeks, weight, and height, were collected. Children's growth status was assessed using the Chinese Child Growth Standards (WS/T 423-2022), where FTT is defined as height and/or weight falling below the 3rd percentile for chronological age and gender.

Laboratory tests, including total protein (TP), albumin (ALB), total bilirubin (TBil), direct bilirubin (DBil), alanine aminotransferase (ALT), aspartate aminotransferase (AST), gamma-glutamyltransferase (GGT), alkaline phosphatase (ALP), total bile acids (TBA), adenosine deaminase (ADA), urea, total triglyceride (TG), and total cholesterol (TC), were performed by the hospital laboratory department.

Treatment and management

NICCD patients were typically treated with lactose-free, MCT-enriched therapeutic formulas and fat-soluble vitamin supplementation. Most patients achieve clinical and biochemical recovery by the age of one year. At that point, diets tailored to the patient's preferences, including low-carbohydrate, protein-enriched, and lipid-enriched content, were introduced. Periodic monitoring of plasma citrulline concentrations, along with other laboratory and physical assessments, was recommended during the post-NICCD phase.

Metabolomics analysis

Serum samples from NICCD, post-NICCD, and their matched controls were collected and stored at -80°C. Metabolomics analysis quantified amino acids, free fatty acids, organic acids, and acylcarnitines. Amino acids and free fatty acids were analyzed using an API4500 liquid chromatography-tandem mass spectrometry (LC-MS/MS) system (Triple Quad™ 4500MD, AB Sciex, MA, USA), while organic acids and acylcarnitines were analyzed using a ultra-performance liquid chromatography-XEVO TQS (UPLC-XEVO TQS) system (Waters, USA). Detailed methods are available in the Supplementary file.

For amino acids and free fatty acids, 2 mL of fasting venous blood was centrifuged at 3000 g for 15 min within 2 h of collection. Fifty microliters of serum were mixed with 200 μL of 0.1% FA methanol containing internal standards and 20 mg/mL DTT, vortexed, centrifuged at 14,000 rpm for 10 min at 4 °C, dried under nitrogen, and reconstituted in 100 μL of a 1:2.5 solvent mixture (70% ACN). Chromatographic separation was performed using an ACQUITY UPLC BEH Amide Column (45 °C) for amino acids and an ACQUITY UPLC BEH C18 Column (35 °C) for fatty acids. Detection was in positive (amino acids) and negative (fatty acids) ion modes with scheduled sMRM.

For organic acids and acylcarnitines, the experimental procedure included the preparation of standard and internal standard mixed solutions, with the standard solution used to establish calibration curves and the internal standard solution applied for error correction. Serum samples were pre-treated by adding 50 μL of serum and 100 μL of internal standard working solution per well, followed by vortex mixing and centrifugation at 4 °C and 5000 rpm for 10 min. The supernatant was transferred to a new plate and dried under nitrogen gas.

Subsequently, 100 μL of ultrapure water was added for reconstitution, mixed thoroughly, and centrifuged again to remove residual particulates. Samples were analyzed using UPLC-MS with an ACQUITY UPLC HSS T3 column for separation under gradient elution, using 0.2% formic acid in water (mobile phase A) and 90% methanol + 10% isopropanol (mobile phase B). The quantification of organic acids and acylcarnitines was performed in negative ion mode (ES-) based on calibration curves.

Data processing

Data were processed through normalization, scaling, and filtering (removal of metabolites with more than 50% missing values), and statistical analysis using MetaboAnalyst 6.0 (www.metaboanalyst.ca), a web-based platform for comprehensive metabolomics data analysis and visualization. Orthogonal partial least squares discriminant analysis (OPLS-DA) was applied to identify differentially expressed metabolites (DEMs) among different groups. The metabolites with variable importance in projection (VIP) exceeding 1, fold change (FC, including up-regulation or down-regulation) ≥ 1.5, and $p < 0.05$ were considered the DEMs. Furthermore, KEGG (https://www.kegg.jp/) was utilized for the pathway analysis. Missing values were estimated by replacing them with small values (half of the minimum positive value in the original data).

Feature selection and model development

Feature selection was conducted from all detected metabolites to ensure a comprehensive and unbiased screening process. Lasso regression was used to identify metabolites associated with FTT by applying a regularization penalty to minimize overfitting and select key variables. Cross-validation determined the optimal regularization parameter (lambda), and metabolites with non-zero coefficients were considered significant. Simultaneously, a random forest (RF) model was built to evaluate variable importance. The optimal number of trees was 500, and two variables were randomly selected to split at each node in this model, determined through a grid search optimization approach.

The intersecting metabolites from the Lasso regression and the RF analysis were selected as potential biomarkers. These biomarkers were used to construct a predictive nomogram, with model performance assessed by plotting the receiver operating characteristic (ROC) curve and calculating the area under the curve (AUC). Internal validation was performed using an enhanced Bootstrap method, and a Calibration curve was generated to evaluate model accuracy. External validation from an additional 9 post-NICCD patients with normal growth.

Statistical analysis

Statistical analysis was performed using IBM SPSS 26.0 (Chicago, IL, USA) and RStudio (R version 4.4.1). Continuous variables with non-normal distributions were expressed as the median (interquartile range) and compared between groups using the Mann-Whitney U test. The "glmnet" package was used for Lasso regression, the "randomForest" package for developing RF models, the "pROC" package for conducting ROC analysis and calculating AUC values, and the "rms" package for nomogram visualization. A p-value < 0.05 was considered statistically significant.

Results.

Clinical characteristics

The demographics of NICCD patients, NICCD-matched controls, post-NICCD patients, and post-NICCD-matched controls are summarized in Table 1. The birth weight of NICCD patients was significantly lower than that of matched controls ($P < 0.05$). No significant differences were observed in age, gender distribution, and gestational age between NICCD patients and matched controls. Similarly, there were no significant differences in age or gender between post-NICCD patients and their matched controls.

Table 2 presents the biochemical indicators for NICCD and post-NICCD patients. In NICCD patients, all showed significantly elevated Tbil, Dbil, and TBA, and over half of the patients exhibited increased GGT and ALP levels, along with decreased TP and ALB levels. Additionally, one patient had elevated TG, and two patients had elevated TC. In post-NICCD patients, all liver function indicators returned to normal ranges. However, elevated TG was observed in 7 patients, and elevated TC was noted in 9 patients.

Table 1 Patients' characteristics of NICCD, post-NICCD, and their matched controls

	NICCD (*N* = 16)	NICCD-matched controls (*N* = 31)	post-NICCD (*N* = 34)	post-NICCD-matched controls (*N* = 70)
Age (months)	0.00(0.00,1.00)	1.00(0.00,2.00)	77.5(45.75,101.5)	75.00(77.00,78.00)
Gender(male/female)	7/9	17/14	16/18	37/33
Birth weight(kg)	2.71(2.36,2.89)*	3.13(2.80,3.34)	3.00(2.63,3.30)	-
Gestational weeks	38(38,39)	39(38,40)	38.5(38,40)	-

*NICCD vs. NICCD matched controls, $P < 0.05$

Table 2 Biochemistry indicators of NICCD and post-NICCD

	NICCD(*N* = 16) medians (interquartile range)	Reference intervals for 10–30 days	post-NICCD(*N* = 34) medians (interquartile range)	Reference intervals for > 12 months
TP(g/L)	43.00(39.13,45.38)	41–63	70.15(68.38,71.83)	61–79
ALB(g/L)	27.50(25.18,29.25)	28–44	44.15(42.6,45.93)	39–54
TBil(umol/L)	110.95(77.48,159.85)	5–21	8.10(6.98,10.30)	5–21
DBil(umol/L)	24.35(18.58,34.73)	0-5.1	1.45(1.20,1.70)	0-5.1
ALT(U/L)	28.5(17.5,39.75)	5–50	13.5(11.00,15.00)	< 50
AST(U/L)	65(42.5,110.25)	25–75	29.00(25.00,33.00)	14–44
GGT(U/L)	223.00(121.75,263.75)	8–57	15.00(12.00,16.50)	5–19
ALP(U/L)	791.00(555.00,1404.25)	42–362	251.50(216.75,285.50)	143–406
ADA(U/L)	6.50(5.00,10.68)	0–15	11.00(9.58,13.08)	0–24
TBA (umol/L)	200.80(135.2,277.5)	0–12	4.35(1.93,6.03)	0–13
Urea(mmol/L)	3.16(2.94,3.48)	1.79–6.43	5.87(5.27,6.77)	2.5–6.5
TG (mmol/L)	1.11(0.55,1.11)	< 1.7	0.93(0.65,1.57)	< 1.7
TC (mmol/L)	3.56(2.57,3.56)	3-5.7	5.38(4.87,5.72)	3-5.7

Altered metabolites and pathways in NICCD and post-NICCD patients

Of the 140 metabolites analyzed, 127 were successfully quantified using LC-MS/MS or UPLC-MS/MS in all subjects. These included 43 amino acid-related metabolites, 34 acylcarnitines, 28 organic acids, and 22 free fatty acids. OPLS-DA showed clear clustering within the same groups and distinct separation between different groups. The NICCD patients were separated from matched controls (Fig. 1A), indicating significant metabolic disturbances in NICCD patients. The volcano plot (FC = 1.5, $p < 0.05$) identified 58 DEMs, of which 42 were upregulated and 16 were downregulated (Fig. 1B). Based on VIP > 1, 46 DEMs were finally identified and were visually demonstrated in the hierarchical cluster analysis heatmap (Fig. 1C). The enrichment pathway analysis was carried out to visualize the metabolic pathways affected in NICCD patients (Fig. 1D). The pathway enrichment analysis demonstrated that: (1) glycine, serine, and, threonine metabolism (2) arginine biosynthesis (3) cysteine and methionine metabolism (4) valine, leucine, and isoleucine biosynthesis (5) arginine and proline metabolism (6) phenylalanine, tyrosine and tryptophan biosynthesis were the top six significant enriched pathways.

The post-NICCD patients were also separated from matched controls (Fig. 2A), and the volcano plot (FC = 1.5, $p < 0.05$) identified 43 DEMs, of which 36 were upregulated, and 7 were downregulated (Fig. 2B). Based on VIP > 1, 33 DEMs were finally identified and were visually demonstrated in the hierarchical cluster analysis heatmap (Fig. 2C). The pathway enrichment analysis (Fig. 2D) demonstrated that (1) biosynthesis of unsaturated fatty acids (2) valine, leucine, and isoleucine biosynthesis (3) valine, leucine, and isoleucine degradation (4) phenylalanine, tyrosine, and tryptophan biosynthesis were the significantly enriched pathways.

Identification of residual metabolite in post-NICCD patients

In the next step, we intersected the DEMs identified in NICCD and post-NICCD patients, initially identifying 13 key metabolites for further analysis: 2-hydroxyisovaleric acid, alpha-ketoisovaleric acid, C5:1, 3-methyl-2-oxovaleric acid, C18:1OH, C20:4, myristic acid, eicosapentaenoic acid (EPA), carnosine, hydroxylysine, phenylpyruvic acid, 2-methylcitric acid, and phenyllactic acid (Fig. 3). These metabolites were significantly altered during NICCD and remained abnormal during post-NICCD, suggesting residual metabolic disruptions or incomplete metabolic recovery. Phenyllactic acid was excluded as its FC indicated elevated levels during NICCD (FC > 1) but decreased to below controls in post-NICCD (FC < 1). Consequently, 12 metabolites were identified as residual markers (Table 3).

Predictors of FTT in Post-NICCD patients

The demographic and biochemical data for the 12 post-NICCD patients in the FTT group and the 22 patients in the normal growth group are presented in Table 4. No significant differences were found in demographics and biochemistry between the two groups ($P > 0.05$). Detailed anthropometric indices of post-NICCD children exhibiting FTT are provided in the supplementary file (Table S1).

All 127 detected metabolites were screened using Lasso regression, and the tuning parameter λ was validated using the ten-fold crossover method (Fig. 4A). Metabolites with non-zero regression coefficients were considered strongly associated with FTT in post-NICCD patients. To achieve a more streamlined model while maintaining interpretability, the model chose lambda.1se (Fig. 4B), and finally, five variables with non-zero regression coefficients were identified at lambda.1se: arginine

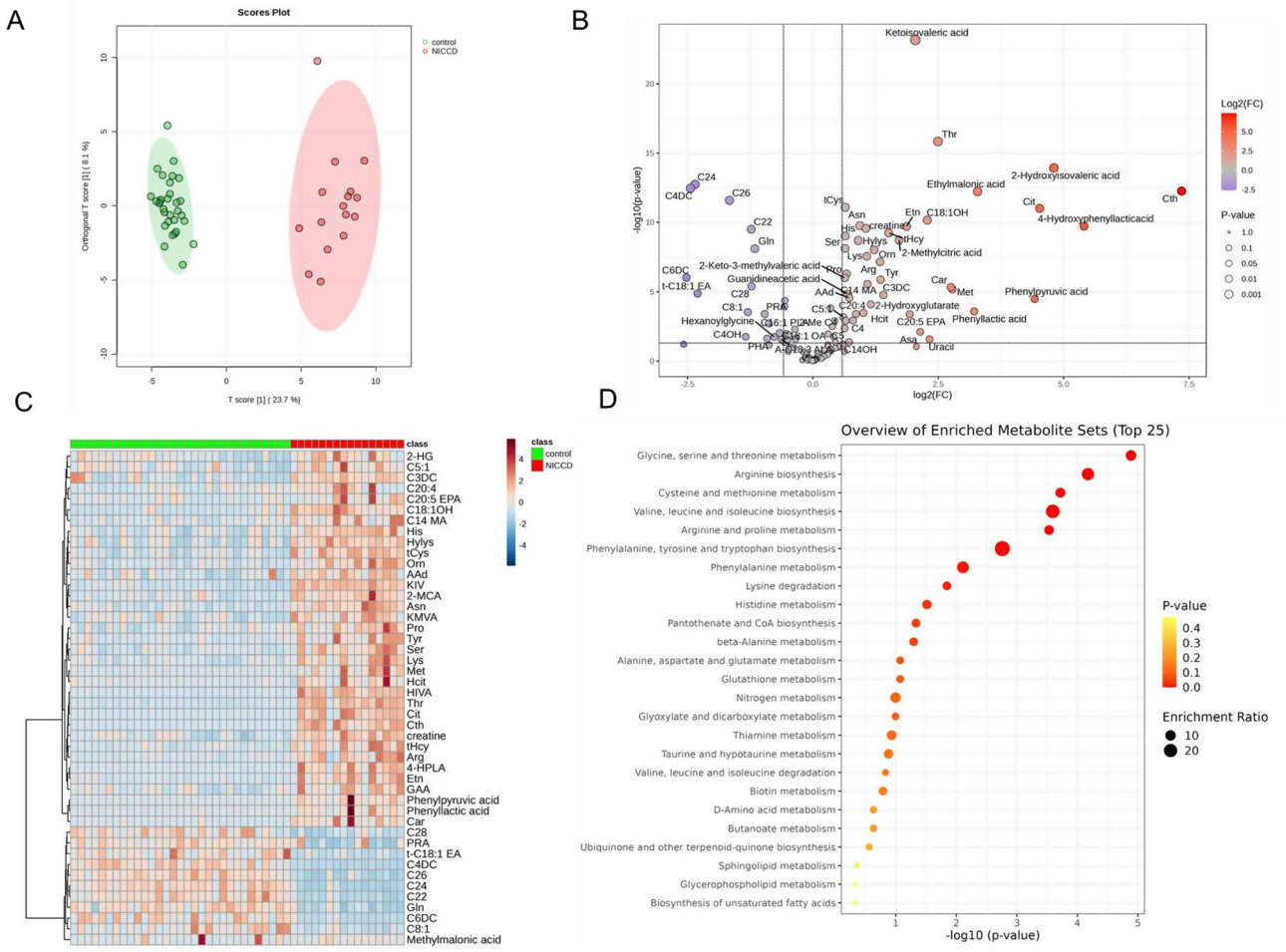

Fig. 1 Serum metabolomic signature in NICCD. (**A**) OPLS-DA score plots showing clustering and dispersion between NICCD vs. controls (**B**) Volcano plot of DEMs with upregulated (red), downregulated (blue), and non-significant metabolites (gray). (**C**) Hierarchical cluster analysis heatmaps of DEMs. (**D**) Enrichment analysis. 2-HG, 2-Hydroxyglutarate; KIV, Ketoisovaleric acid; 2-MCA, 2-Methylcitric acid; KMVA, 2-Keto-3-methylvaleric acid; HIVA, 2-Hydroxyisovaleric acid; 4-HPLA, 4-Hydroxyphenyllactic acid; GAA, Guanidineacetic acid

(Arg), alanine (Ala), aspartate (Asp), kynurenine (Kyn), and ethanolamine.

Additionally, an RF was applied to analyze all 127 metabolites. The out-of-bag (OOB) error rate was 26.47% (Fig. 4C). Variable importance was ranked based on the Mean Decrease in Gini score, and the top ten most influential variables were presented (Fig. 4D). Four variables, Arg, Ala, Asp, and Kyn, were found to overlap between the Lasso-selected variables and the top ten variables ranked by RF.

Model development and validation

The model, developed using Arg, Ala, Asp, and Kyn with their respective coefficients, was visualized as a nomogram (Fig. 5). In this system, decreases of 5 μmol/L in Asp, 0.2 μmol/L in Kyn, 10 μmol/L in Arg, and 50 μmol/L in Ala increased the score by 1.28, 9.09, 5.04, and 3.03 points, respectively. ROC analysis showed an AUC of 0.947 (95% CI: 0.871-1, $P<0.001$), indicating excellent discriminatory performance (Fig. 6A). Internal validation using 500 Bootstrap resamples resulted in an AUC of 0.944, with minimal overestimation (0.003), confirming strong model discrimination. The Calibration curve (Fig. 6B) and Hosmer-Lemeshow test ($P=0.86$) indicated adequate agreement between predicted and actual probabilities. External validation from an additional 9 post-NICCD patients with normal growth showed that 8 patients were correctly classified as low risk (probability < 0.5), while 1 patient were classified as high risk (probability > 0.5), demonstrated a specificity of 88.9% and a false positive rate of 11.1% in this validation cohort (Table S2).

Discussion

In this study, we identified the biosynthesis of unsaturated fatty acids as a key metabolic pathway in post-NICCD patients, along with 12 residual metabolites significantly altered during both NICCD and post-NICCD phases.

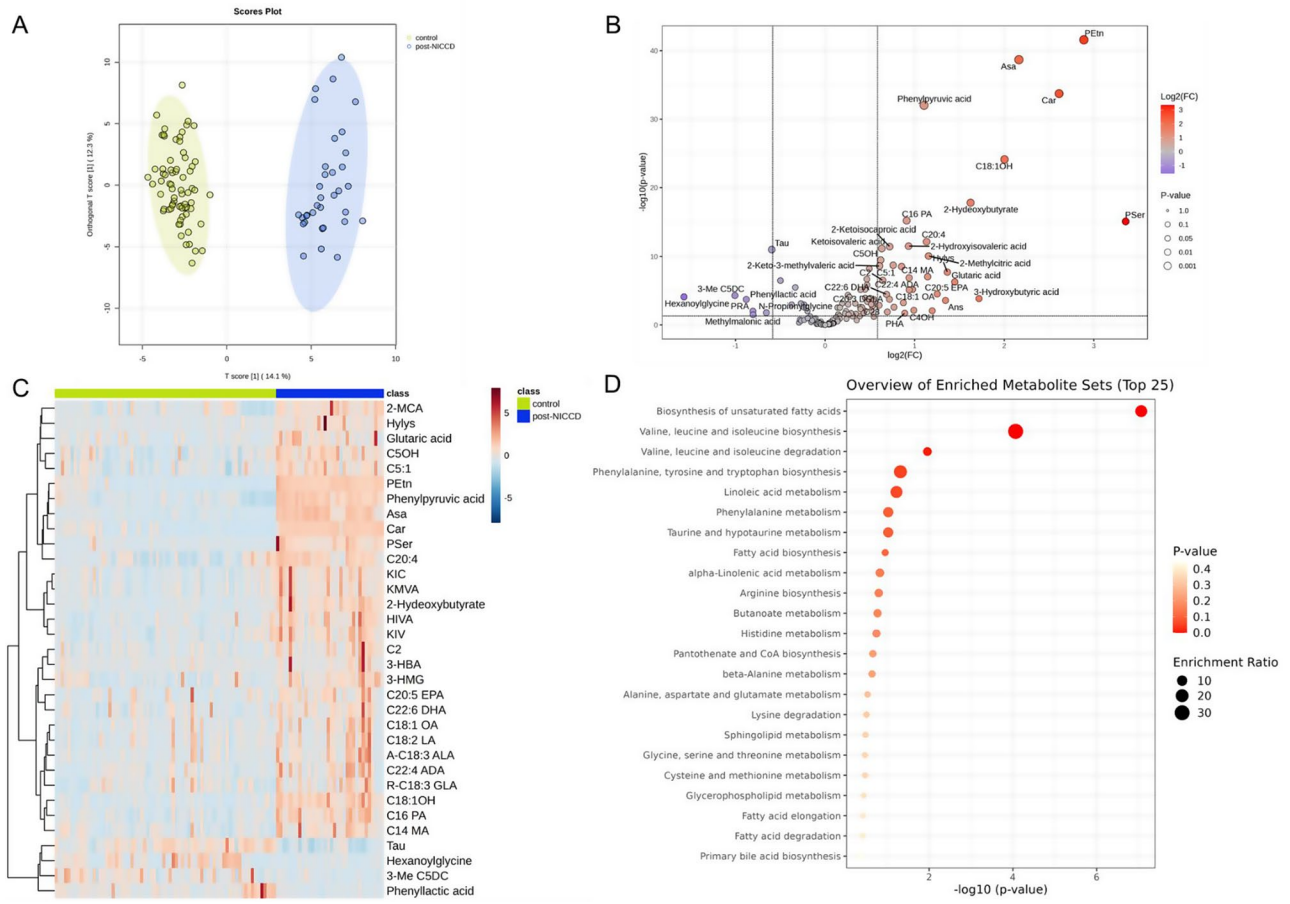

Fig. 2 Serum metabolomic signature in post-NICCD. (**A**) OPLS-DA score plots showing clustering and dispersion between post-NICCD vs. controls. (**B**) Volcano plot of DEMs with upregulated (red), downregulated (blue), and non-significant metabolites (gray). (**C**) Hierarchical cluster analysis heatmaps of DEMs. (**D**) Enrichment analysis. 2-MCA, 2-Methylcitric acid; KIC, 2-Ketoisocaproic acid; KMVA, 2-Keto-3-methylvaleric acid; HIVA, 2-Hydroxyisovaleric acid; KIV, Ketoisovaleric acid; 3-HBA, 3-Hydroxybutyric acid; 3-HMG, 3-Hydroxy-3-Methylglutaric acid

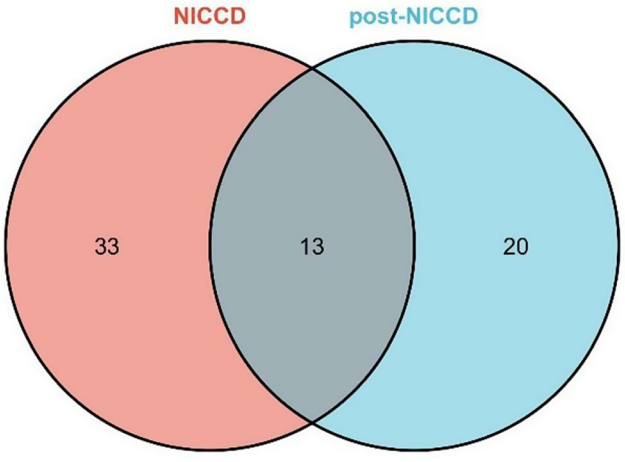

Fig. 3 Intersection of DEMs in NICCD and post-NICCD

These findings indicate that metabolic recovery remains incomplete despite the normalization of liver function markers and clinical symptoms. Some post-NICCD patients exhibit FTT. Using machine learning models,

Table 3 Fold change of NICCD vs. matched control and post-NICCD vs. matched control

	NICCD vs. matched control	Post-NICCD vs. matched control
Carnosine	6.723	6.114
Phenylpyruvic acid	21.435	2.152
C18:1OH	4.860	4.007
C20:4	1.813	2.193
2-Hydroxyisovaleric acid	27.949	1.908
alpha-Ketoisovaleric acid	4.120	1.551
2-Methylcitric acid	3.293	2.228
Myristic acid	2.128	1.808
C5:1	1.524	1.693
3-Methyl-2-oxovaleric acid	1.554	1.525
Hydroxylysine	1.872	2.576
Eicosapentaenoic acid	3.815	2.382
Phenyllactic acid	9.292	0.543

Table 4 Demographics and biochemistry of the post-NICCD patients in the FTT and normal growth

	FTT (*N* = 12)	Normal growth (*N* = 22)	*P*
Patients' characteristics			
Age(months)	74.5(41.0,87.0)	77.5(45.75,111.25)	0.40
Gender(male/female)	7/5	9/13	0.33
Birth weight(kg)	2.65(2.30,3.22)	3(2.84, 3.3)	0.15
Gestational weeks	38(38,38.75)	39(38,40)	0.26
Biochemical indicators			
TP	69.90(67.00,71.88)	70.30(68.88,71.83)	0.48
Albumin	43.75(42.45, 45.73)	44.45(43.20,46.03)	0.51
TB	8.10(7.37, 9.55)	8.45(6.35,10.90)	0.84
DB	1.55(1.33,1.68)	1.35(1.00,1.75)	0.42
ALT	13.50(10.25,14.75)	13.50(11.75,16.25)	0.40
AST	32.00(27.15,35.00)	28.00(23.75,32.25)	0.07
GGT	14.00(11.25,17.50)	15.50(12.75,16.50)	0.51
ALP	227.50(231.75,259.25)	261.50(222.50,301.50)	0.16
ADA	11.00(9.00,14.20)	10.95(9.83,13.00)	0.94
TBA	4.40(1.55,5.83)	4.35(2.45,6.10)	0.64
Urea	5.81(5.14,6.74)	5.98(5.32,6.77)	0.89
TG	0.84(0.59,1.17)	1.09(0.81,1.79)	0.07
TC	5.31(4.80,5.46)	5.41(4.87,5.94)	0.41

Kyn, Arg, Ala, and Asp were identified as predictive biomarkers, developing a non-invasive risk assessment tool.

Citrin deficiency reduces liver cytosolic aspartate, a key substrate for argininosuccinate synthetase (ASS) in the urea cycle, leading to the accumulation of citrulline (a direct substrate of ASS) and ornithine (an upstream substrate in the same cycle). Arginine, a downstream product of ASS [19], is primarily synthesized from citrulline in the kidneys and small intestine [20]. The accumulation of citrulline in NICCD enhances this extrahepatic synthesis, resulting in elevated arginine levels. In addition to disrupted arginine biosynthesis, other amino acid pathways, including glycine-serine-threonine, methionine, BCAA, and aromatic amino acid metabolism, were also affected. These findings align with decreased levels of glycine along with elevated levels of methionine, tyrosine, and phenylalanine in NBS, in addition to urea cycle-related amino acids [21].

During the post-NICCD phase, most patients experienced significant improvements in cholestasis, citrullinemia, and clinical symptoms within the first year. However, some patients exhibited hyperlipidemia, which may be attributed to factors such as a high-lipid diet,

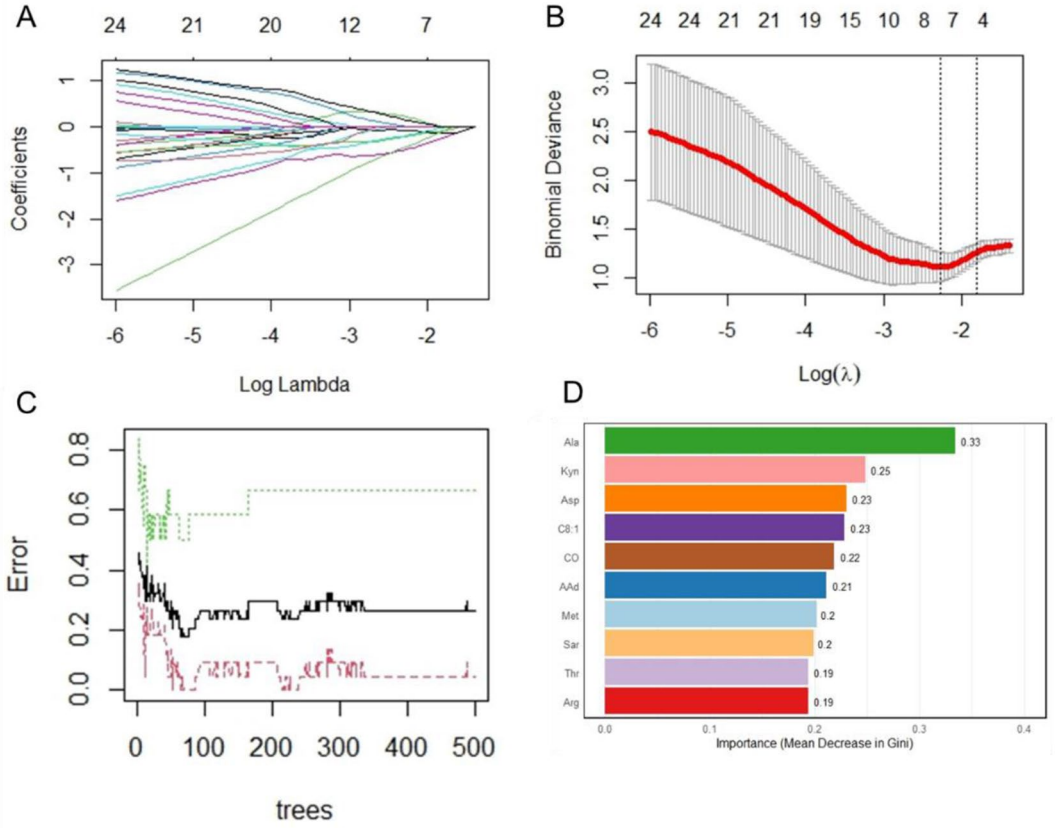

Fig. 4 Machine learning screening. (**A**) Lasso regression coefficient path plot. (**B**) Cross-validation error plot. The two dashed lines represent lambda.min(left), the value of lambda that minimizes the cross-validated error, and lambda.1se(right), the largest lambda within one standard error of lambda.min, providing a simpler model. (**C**) The choice of the number of mtry and ntree. The red line shows the error rate for the negative class, the green line for the positive class, and the black line for the out-of-bag error. (**D**) Variable importance plot for the RF model (top 10)

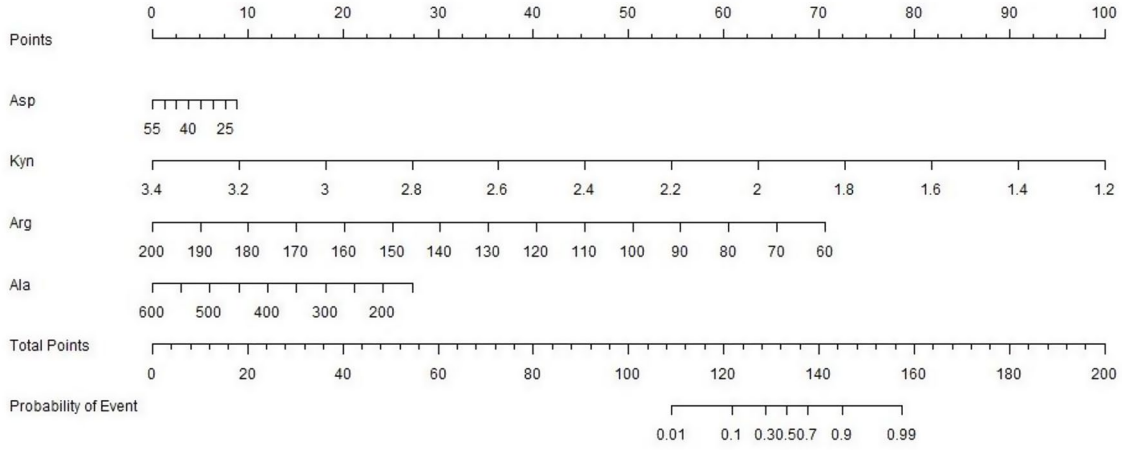

Fig. 5 Nomogram visualization

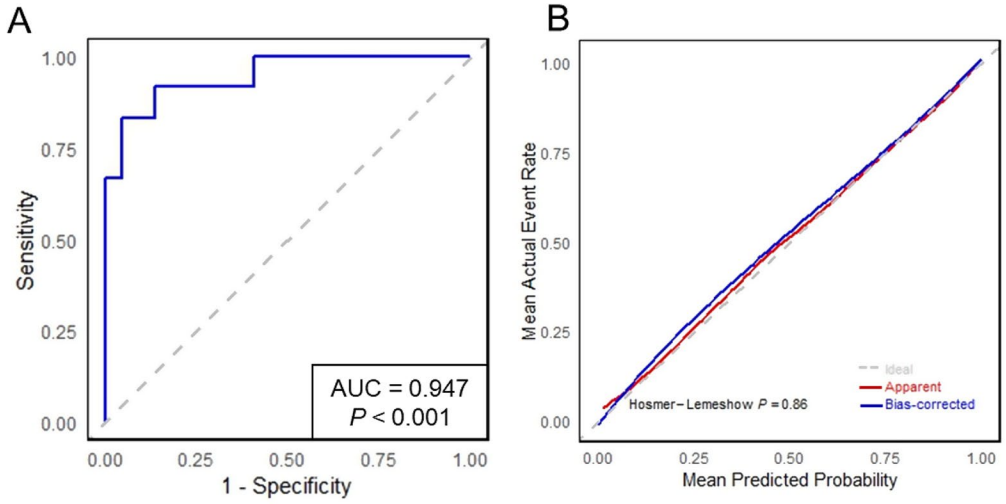

Fig. 6 ROC (**A**) and Calibration (**B**) curve for predicting FTT in post-NICCD patients

increased expression of liver HMG-CoA reductase leading to enhanced cholesterol synthesis [12], high carbohydrate meals, and failure to thrive and dyslipidemia caused by citrin deficiency (FTTDCD) due to poor control [5, 22]. The impairment of the malate-aspartate shuttle disrupts hepatic glycolysis and de novo lipogenesis, which leads to secondary downregulation of fatty acid oxidation through the suppression of peroxisome proliferator-activated receptor α (PPARα) [4, 23]. Our study revealed significant enrichment of unsaturated fatty acid biosynthesis in post-NICCD patients. This indicates that the suppressed fatty acid oxidation primarily contributes to the accumulation of unsaturated fatty acids, including palmitic acid, gamma-linolenic acid, oleic acid, linoleate, EPA, and docosahexaenoic acid. These metabolites may contribute to the elevated triglyceride and cholesterol levels observed in some post-NICCD patients, further indicating that impaired malate/aspartate shuttle in post-NICCD patients has not achieved ideal control.

Twelve intersecting DEMs significantly altered in the NICCD and post-NICCD phases were defined as residual metabolites. While most of the fold changes decreased in the post-NICCD period compared to NICCD, these metabolites remained among the most abnormal compared to controls. This indicates the presence of long-term metabolic residues and suggests that metabolic abnormalities in CD patients persist despite treatment. 2-Hydroxyisovaleric acid, α-ketosovaleric acid, 3-methyl-2-oxovaleric acid, and C5:1 are intermediate products of BCAAs metabolism. Their sustained elevation reflects ongoing dysfunction in BCAA metabolism. This aligns with previous findings of increased ketogenic amino acids, BCAAs, and β-alanine levels, alongside decreased glucogenic amino acids, during the asymptomatic phase of CD [11]. Since BCAAs are primarily metabolized in skeletal muscles for energy production [24], disruptions in their metabolism may further aggravate energy deficiencies in both NICCD and post-NICCD periods.

Long-chain acylcarnitines (C18:1OH and C20:4) and free fatty acids (myristic acid and EPA) were also identified as residual metabolites. During the NICCD period, CD impairs fatty acid β-oxidation, leading to energy deficiency and dysfunction of energy-dependent bile canalicular transporters [25]. This disruption hampers bile excretion from hepatocytes, resulting in cholestasis. Cholestasis further inhibits the activation of long-chain fatty acids (e.g., dysfunction of palmitoyl-CoA synthase and carnitine palmitoyltransferase II (CPT II), causing elevated levels of long-chain acylcarnitines and fatty acids [26]. In the post-NICCD period, although liver function markers have normalized, incomplete recovery of fatty acid β-oxidation may lead to residual cholestasis, impairing palmitoyl-CoA synthase and CPT II function. As a result, long-chain acylcarnitines and fatty acids remain elevated compared to healthy children.

Carnosine, a dipeptide synthesized from β-alanine and histidine, exhibits antioxidant and stress-relieving properties [27]. Studies suggest that CD patients during the silent period experience persistent oxidative stress, potentially due to increased cytosolic NADH [12]. The increase in carnosine may reflect an enhanced antioxidant response. Similarly, elevated hydroxylysine levels indicate abnormal collagen metabolism, characterized by increased collagen breakdown or imbalanced modifications, which may impair bone development [28]. Additionally, phenylpyruvic acid signals disruptions in the phenylalanine pathway, while 2-methylcitric acid is a marker of propionic acid metabolism disorders. Together, these residual metabolites represent key markers for monitoring recovery and identifying patients at risk of long-term complications. They also offer potential therapeutic targets for interventions aimed at improving outcomes in CD during post-NICCD phases.

Besides hyperlipidemia, growth outcomes are also an important physical examination during the post-NICCD period, indicating a long-term prognosis of CD. Previous studies have reported low birth weight in NICCD patients and low body mass index (BMI) in AACD patients [29]. Consistent with these findings, our study confirmed that NICCD patients exhibit significantly lower birth weights due to impaired de novo lipogenesis in the third trimester, which impairs body fat deposition and myelination of the developing central nervous system [30]. In our study, we divided the post-NICCD patients into two groups based on their growth outcomes and identified four optimal predictors for FTT in post-NICCD: Kyn, Arg, Ala, and Asp. Lower levels of these four predictors correlate with increased FTT risk.

Kyn is a critical metabolite in the tryptophan catabolic pathway, playing a vital role in protein synthesis, energy production, and immune regulation [31]. Studies have reported that serum Kyn levels were lower in pregnant women experiencing fetal growth restriction [32]. As a key intermediate, Kyn contributes to NAD + synthesis [33], and its reduction impairs NAD + production, worsening the NAD+/NADH imbalance caused by mitochondrial aspartate-glutamate carrier dysfunction in citrin deficiency. This intensifies the energy crisis. Furthermore, NAD + acts as a cofactor for multiple signaling pathways. For instance, NAD + deficiency affects the Sirtuins signaling pathway, reducing SIRT1 and SIRT3 activity, which impacts mitochondrial biogenesis and function, leading to abnormal energy metabolism [34] and subsequently influencing growth. Arg is effective in addressing hyperammonemia and hypertriglyceridemia [35, 36]. Previous research suggests that the administration of arginine and sodium pyruvate alongside low-carbohydrate meals can serve as an effective therapy for CD patients. This approach helps prolong metabolic normalcy, promote rapid weight and height increases, and offering a more cost-effective alternative to liver transplantation [37]. Arginine supplementation may reduce the elevated oxidative stress in post-NICCD patients and increase the expression of PPARγ coactivator-1α (PGC-1α) [38], which may enhance PPARγ activity and promote mitochondrial fatty acid oxidation. Additionally, arginine activates the mTOR signaling pathway [39], stimulating protein synthesis and cell proliferation, thereby supporting growth and development.

Glucogenic amino acids play a critical role in glucose homeostasis in citrin deficiency. Since lactate-based gluconeogenesis is impaired [40], post-NICCD patients maintain normal blood glucose levels primarily through gluconeogenesis from alanine and other glucogenic amino acids [11]. When alanine levels decrease in post-NICCD patients, the reduced availability of gluconeogenic substrates may result in hypoglycemia. This chronic hypoglycemia can subsequently impair growth and development by disrupting important signaling pathways such as GH/IGF-1 [41]. Citrin deficiency impairs mitochondrial aspartate transport to the cytosol, reducing cytosolic aspartate levels. As aspartate is a critical precursor for purine and pyrimidine nucleotide synthesis, its decreased availability limits nucleotide production [42]. Post-NICCD patients experience elevated oxidative stress, causing DNA damage that requires sufficient nucleotides for repair. Under aspartate deficiency, compromised DNA damage repair activates the p53 pathway, leading to cell cycle arrest or apoptosis and affecting tissue growth [43]. This nucleotide synthesis impairment likely underlies growth retardation in citrin deficiency patients.

Monitoring and replenishing Kyn, Arg, Ala, and Asp levels may represent a promising strategy to improve growth outcomes in affected individuals. Zinc supplementation should also be encouraged, especially in

individuals with a marked failure to thrive [30]. The predictive model for FTT in post-NICCD patients, constructed using these four biomarkers, is characterized by easily accessible data, straightforward implementation, and strong diagnostic performance. It effectively meets clinical needs by identifying high-risk patients and enabling timely interventions, making it highly suitable for widespread application. In medical institutions where metabolomics analysis is not available, we recommend that clinical practice incorporate regular monitoring of growth velocity (e.g., dynamic changes in height/weight Z-scores, BMI), serum lipid profiles (including total cholesterol, triglycerides, HDL, and LDL), and nutritional status assessments (such as protein and fat intake, dietary patterns). A combination of growth trajectory evaluation and routine biochemical monitoring may serve as a practical approach to identify post-NICCD patients at risk for FTT, allowing for timely intervention.

This study has several strengths. First, we demonstrated that despite clinical and biochemical recovery, post-NICCD patients maintain incomplete metabolic profiles with 12 identified residual metabolites. Additionally, we found that the primary altered metabolic pathways in the post-NICCD period differ from those in the NICCD stage. Finally, we identified four biomarkers predictive of FTT in post-NICCD, constructing a risk assessment tool and providing a foundation for further research into the metabolic mechanisms of FTT and potential therapeutic targets. However, due to the rarity of NICCD, this study was limited to cases from Zhejiang Province, and the relatively small sample size may impact the model's generalizability. Our external validation only included post-NICCD patients with normal growth; therefore, larger multicenter cohort studies with a more diverse population are needed to validate our findings and better assess the model's applicability to a broader population. Furthermore, as this research focused on infants and adolescents, future studies should explore metabolic changes in AACD across different age groups.

In summary, this study revealed that although clinical symptoms and liver function of post-NICCD patients return to normal, their metabolic profiles remain incompletely restored. Kyn, Arg, Ala, and Asp were identified as biomarkers for predicting FTT in post-NICCD patients, providing a basis for individualized management and targeted therapeutic strategies.

Abbreviations

NICCD	Neonatal intrahepatic cholestasis from citrin deficiency
CD	Citrin deficiency
Cit	Citrulline
DEMs	Differentially abundant metabolites
BCAAs	Branched-chain amino acids
FTT	Failure to thrive
MCT	Medium-chain triglyceride
FC	Fold change
Arg	Arginine
Ala	Alanine
Asp	Aspartate
Kyn	Kynurenine
EPA	Eicosapentaenoic acid
RF	Random forest

Supplementary Information

The online version contains supplementary material available at https://doi.org/10.1186/s12986-025-00928-x.

Supplementary Material 1

Acknowledgements

We would like to thank Zhejiang Biosan Biochemical Technologies Co., Ltd. for providing the LC-MS/MS and UPLC-MS/MS.

Author contributions

WPY, ZD, and HLW should be considered joint first authors. WPY, ZD, and HLW designed the research, analyzed the data, and wrote the manuscript; WPY and GPP analyzed data and performed bioinformatics analysis, CZY, HZZ, and ZKJ revised the manuscript; HQM, ZKJ, WBQ, and HXW supervised the research study and should be considered joint corresponding authors. All authors approved the final manuscript to be published.

Funding

Xinwen Huang was supported by grants from the National Natural Science Foundation of China (82073560). This work was supported by grants from the "Pioneer" and "Leading Goose" R&D Program of Zhejiang Province (No. 2024C03152 to H.F.). The funders had no role in the design and conduct of the study; collection, management, analysis, and interpretation of the data; preparation, review, or approval of the manuscript; and decision to submit the manuscript for publication. The other authors received no additional funding.

Data availability

Some or all datasets generated during and/or analyzed during the current study are not publicly available regarding patient privacy and confidentiality but are available from the corresponding author upon reasonable request.

Declarations

Ethics approval and consent to participate

This study was approved by the Institutional Review Board of the Ethics Committee in Children's Hospital, Zhejiang University School of Medicine (reference number: 2021-IRB-292). Written consents were obtained from parents for sample collection and data publication.

Consent for publication

We confirm that the family has signed a written informed consent for the publication of their children's genetic data, clinical details, and/or any accompanying images.

Competing interests

The authors declare no competing interests.

Author details

[1]Department of Genetics and Metabolism, Children's Hospital of Zhejiang University School of Medicine, National Clinical Research Center for Child Health, No. 3333 Binsheng Road, Binjiang District, Hangzhou City, Zhejiang Province 310052, China
[2]School of Geography Science and Geomatics Engineering, Suzhou University of Science and Technology, Suzhou 215009, China
[3]Suzhou Bohe Intelligent Information Technology Co., Ltd., Suzhou 215100, China
[4]Human Metabolomics Institute, Inc., Shenzhen, Guangdong 518109, China
[5]Children's Medical Center, Shenzhen Guangming District People's Hospital, Shenzhen, Guangdong 518106, China

[6]Children's Medical Center, University of the Chinese Academy of Sciences-Shenzhen Hospital, Shenzhen, Guangdong, China

Received: 18 December 2024 / Accepted: 22 April 2025
Published online: 12 May 2025

References

1. Lin J, Lin W, Lin Y, Peng W, Zheng Z. Clinical and genetic analysis of 26 Chinese patients with neonatal intrahepatic cholestasis due to Citrin deficiency. Clin Chim Acta. 2024;552:117617.
2. Kido J, Makris G, Santra S, Haberle J. Clinical landscape of Citrin deficiency: A global perspective on a multifaceted condition. J Inherit Metab Dis. 2024;47(6):1144–56.
3. Tavoulari S, Lacabanne D, Thangaratnarajah C, Kunji ERS. Pathogenic variants of the mitochondrial aspartate/glutamate carrier causing Citrin deficiency. Trends Endocrinol Metab. 2022;33(8):539–53.
4. Hayasaka K. Pathogenesis and management of Citrin deficiency. Intern Med. 2024;63(14):1977–86.
5. Okano Y, Ohura T, Sakamoto O, Inui A. Current treatment for Citrin deficiency during NICCD and adaptation/compensation stages: strategy to prevent CTLN2. Mol Genet Metab. 2019;127(3):175–83.
6. Hayasaka K. Metabolic basis and treatment of Citrin deficiency. J Inherit Metab Dis. 2021;44(1):110–7.
7. Vukovic T, Kuek LE, Yu B, Makris G, Haberle J. The therapeutic landscape of Citrin deficiency. J Inherit Metab Dis. 2024;47(6):1157–74.
8. Hayasaka K, Numakura C. Adult-onset type II citrullinemia: current insights and therapy. Appl Clin Genet. 2018;11:163–70.
9. Saheki T, Inoue K, Tushima A, Mutoh K, Kobayashi K. Citrin deficiency and current treatment concepts. Mol Genet Metab. 2010;100:S59–64.
10. Hirayama S, Nagasaka H, Honda A, Komatsu H, Kodama T, Inui A, et al. Cholesterol metabolism is enhanced in the liver and brain of children with Citrin deficiency. J Clin Endocrinol Metab. 2018;103(7):2488–97.
11. Miyazaki T, Nagasaka H, Komatsu H, Inui A, Morioka I, Tsukahara H, et al. Serum amino acid profiling in Citrin-Deficient children exhibiting normal liver function during the apparently healthy period. JIMD Rep. 2019;43:53–61.
12. Nagasaka H, Okano Y, Tsukahara H, Shigematsu Y, Momoi T, Yorifuji J, et al. Sustaining hypercitrullinemia, hypercholesterolemia and augmented oxidative stress in Japanese children with aspartate/glutamate carrier isoform 2-citrin-deficiency even during the silent period. Mol Genet Metab. 2009;97(1):21–6.
13. Arai-Ichinoi N, Kikuchi A, Wada Y, Sakamoto O, Kure S. Hypoglycemic attacks and growth failure are the most common manifestations of Citrin deficiency after 1 year of age. J Inherit Metab Dis. 2021;44(4):838–46.
14. Numakura C, Tamiya G, Ueki M, Okada T, Maisawa Si, Kojima-Ishii K, et al. Growth impairment in individuals with Citrin deficiency. J Inherit Metab Dis. 2019;42(3):501–8.
15. Suryawan A, Jalaludin MY, Poh BK, Sanusi R, Tan VMH, Geurts JM, et al. Malnutrition in early life and its neurodevelopmental and cognitive consequences: a scoping review. Nutr Res Rev. 2022;35(1):136–49.
16. Costanzo M, Zacchia M, Bruno G, Crisci D, Caterino M, Ruoppolo M. Integration of proteomics and metabolomics in exploring genetic and rare metabolic diseases. Kidney Dis (Basel). 2017;3(2):66–77.
17. Kuhara T, Ohse M, Inoue Y, Cooper AJ. A GC/MS-based metabolomic approach for diagnosing Citrin deficiency. Anal Bioanal Chem. 2011;400(7):1881–94.
18. Inui A, Ko JS, Chongsrisawat V, Sibal A, Hardikar W, Chang MH, et al. Update on the diagnosis and management of neonatal intrahepatic cholestasis caused by Citrin deficiency: expert review on behalf of the Asian Pan-Pacific society for pediatric gastroenterology, hepatology, and nutrition. J Pediatr Gastroenterol Nutr. 2024;78(2):178–87.
19. Song YZ, Li BX, Chen FP, Liu SR, Sheng JS, Ushikai M, et al. Neonatal intrahepatic cholestasis caused by Citrin deficiency: clinical and laboratory investigation of 13 subjects in Mainland of China. Dig Liver Dis. 2009;41(9):683–9.
20. Saheki T, Kobayashi K. Mitochondrial aspartate glutamate carrier (citrin) deficiency as the cause of adult-onset type II citrullinemia (CTLN2) and idiopathic neonatal hepatitis (NICCD). J Hum Genet. 2002;47(7):333–41.
21. Zhang T, Zhu S, Miao H, Yang J, Shi Y, Yue Y, et al. Dynamic changes of metabolic characteristics in neonatal intrahepatic cholestasis caused by Citrin deficiency. Front Mol Biosci. 2022;9:939837.
22. Lee BH, Jin HY, Kim GH, Choi JH, Yoo HW. Nonalcoholic fatty liver disease in 2 siblings with adult-onset type II citrullinemia. J Pediatr Gastroenterol Nutr. 2010;50(6):682–5.
23. Komatsu M, Kimura T, Yazaki M, Tanaka N, Yang Y, Nakajima T, et al. Steatogenesis in adult-onset type II citrullinemia is associated with down-regulation of PPARalpha. Biochim Biophys Acta. 2015;1852(3):473–81.
24. Plotkin DL, Delcastillo K, Van Every DW, Tipton KD, Aragon AA, Schoenfeld BJ. Isolated leucine and Branched-Chain amino acid supplementation for enhancing muscular strength and hypertrophy: A narrative review. Int J Sport Nutr Exerc Metab. 2021;31(3):292–301.
25. Song YZ. Pathophysiologic and therapeutic insights into neonatal intrahepatic cholestasis caused by Citrin deficiency: focusing on the canalicular transporters. Chin J Appl Clin Pediatr. 2018;33(19):1447–49.
26. Lee NC, Chien YH, Kobayashi K, Saheki T, Chen HL, Chiu PC, et al. Time course of acylcarnitine elevation in neonatal intrahepatic cholestasis caused by Citrin deficiency. J Inherit Metab Dis. 2006;29(4):551–5.
27. Boldyrev AA, Aldini G, Derave W. Physiology and pathophysiology of carnosine. Physiol Rev. 2013;93(4):1803–45.
28. Rauch F, Georg M, Stabrey A, Neu C, Blum WF, Remer T, et al. Collagen markers Deoxypyridinoline and hydroxylysine glycosides: pediatric reference data and use for growth prediction in growth hormone-deficient children. Clin Chem. 2002;48(2):315–22.
29. Kido J, Haberle J, Sugawara K, Tanaka T, Nagao M, Sawada T, et al. Clinical manifestation and long-term outcome of Citrin deficiency: report from a nationwide study in Japan. J Inherit Metab Dis. 2022;45(3):431–44.
30. Saheki T, Song Y-Z. Citrin deficiency. Seattle (WA): University of Washington, Seattle; 2005.
31. Savitz J. The kynurenine pathway: a finger in every pie. Mol Psychiatry. 2020;25(1):131–47.
32. Yaman S, Ceyhan M, Hancerliogullari N, Koc EM, Candar T, Tokmak A. Serum levels of kynurenine in pregnancies with fetal growth restriction and oligohydramnios. J Perinat Med. 2023;51(5):641–5.
33. Castro-Portuguez R, Sutphin GL. Kynurenine pathway, NAD(+) synthesis, and mitochondrial function: targeting Tryptophan metabolism to promote longevity and healthspan. Exp Gerontol. 2020;132:110841.
34. Haigis MC, Sinclair DA. Mammalian sirtuins: biological insights and disease relevance. Annu Rev Pathol. 2010;5:253–95.
35. Saheki T, Inoue K, Tushima A, Mutoh K, Kobayashi K. Citrin deficiency and current treatment concepts. Mol Genet Metab. 2010;100(Suppl 1):S59–64.
36. Imamura Y, Kobayashi K, Shibatou T, Aburada S, Tahara K, Kubozono O, et al. Effectiveness of carbohydrate-restricted diet and arginine granules therapy for adult-onset type II citrullinemia: a case report of siblings showing homozygous SLC25A13 mutation with and without the disease. Hepatol Res. 2003;26(1):68–72.
37. Mutoh K, Kurokawa K, Kobayashi K, Saheki T. Treatment of a citrin-deficient patient at the early stage of adult-onset type II citrullinaemia with arginine and sodium pyruvate. J Inherit Metab Dis. 2008;31(Suppl 2):S343–7.
38. Wu G, Meininger CJ, McNeal CJ, Bazer FW, Rhoads JM. Role of L-Arginine in nitric oxide synthesis and health in humans. Adv Exp Med Biol. 2021;1332:167–87.
39. Ma X, Han M, Li D, Hu S, Gilbreath KR, Bazer FW, et al. L-Arginine promotes protein synthesis and cell growth in brown adipocyte precursor cells via the mTOR signal pathway. Amino Acids. 2017;49(5):957–64.
40. Sinasac DS, Moriyama M, Jalil MA, Begum L, Li MX, Iijima M, et al. Slc25a13-knockout mice harbor metabolic deficits but fail to display hallmarks of adult-onset type II citrullinemia. Mol Cell Biol. 2004;24(2):527–36.
41. Senniappan S, Hussain K. An evaluation of growth hormone and IGF-1 responses in neonates with hyperinsulinaemic hypoglycaemia. Int J Endocrinol. 2013;2013:638257.
42. Lane AN, Fan TW. Regulation of mammalian nucleotide metabolism and biosynthesis. Nucleic Acids Res. 2015;43(4):2466–85.
43. Williams AB, Schumacher B. p53 in the DNA-Damage-Repair process. Cold Spring Harb Perspect Med. 2016;6(5).

Publisher's note